ARL

An Automated Energy Detection Algorithm Based on Morphological and Statistical Processing Techniques

by Kwok F Tom

NOTICES

Disclaimers

The findings in this report are not to be construed as an official Department of the Army position unless so designated by other authorized documents.

Citation of manufacturer's or trade names does not constitute an official endorsement or approval of the use thereof.

Destroy this report when it is no longer needed. Do not return it to the originator.

US Army Research Laboratory

An Automated Energy Detection Algorithm Based on Morphological and Statistical Processing Techniques

by Kwok F Tom
Sensors and Electron Devices Directorate, ARL

REPORT DOCUMENTATION PAGE		*Form Approved* *OMB No. 0704-0188*

Public reporting burden for this collection of information is estimated to average 1 hour per response, including the time for reviewing instructions, searching existing data sources, gathering and maintaining the data needed, and completing and reviewing the collection information. Send comments regarding this burden estimate or any other aspect of this collection of information, including suggestions for reducing the burden, to Department of Defense, Washington Headquarters Services, Directorate for Information Operations and Reports (0704-0188), 1215 Jefferson Davis Highway, Suite 1204, Arlington, VA 22202-4302. Respondents should be aware that notwithstanding any other provision of law, no person shall be subject to any penalty for failing to comply with a collection of information if it does not display a currently valid OMB control number.
PLEASE DO NOT RETURN YOUR FORM TO THE ABOVE ADDRESS.

1. REPORT DATE *(DD-MM-YYYY)*	2. REPORT TYPE	3. DATES COVERED (From - To)
January 2018	Technical Report	1 October 2016–30 September 2017

4. TITLE AND SUBTITLE	5a. CONTRACT NUMBER
An Automated Energy Detection Algorithm Based on Morphological and Statistical Processing Techniques	
	5b. GRANT NUMBER
	5c. PROGRAM ELEMENT NUMBER
6. AUTHOR(S)	5d. PROJECT NUMBER
Kwok F Tom	
	5e. TASK NUMBER
	5f. WORK UNIT NUMBER

7. PERFORMING ORGANIZATION NAME(S) AND ADDRESS(ES)	8. PERFORMING ORGANIZATION REPORT NUMBER
US Army Research Laboratory ATTN: RDRL-SER-E 2800 Powder Mill Road Adelphi, MD 20783-1138	ARL-TR-8272

9. SPONSORING/MONITORING AGENCY NAME(S) AND ADDRESS(ES)	10. SPONSOR/MONITOR'S ACRONYM(S)
	11. SPONSOR/MONITOR'S REPORT NUMBER(S)

12. DISTRIBUTION/AVAILABILITY STATEMENT
Approved for public release; distribution is unlimited.

13. SUPPLEMENTARY NOTES

14. ABSTRACT
This report is the result of applying morphological image and statistical processing techniques to the energy detection scenario of signals in the RF spectrum domain. The algorithm automatically establishes a detection threshold based on the data of the RF spectrum measurement. It is able to determine the threshold level even when there are signals present in the RF spectrum.

15. SUBJECT TERMS
RF spectrum, morphological imaging processing, detection threshold algorithm, erosion, dilation, opening

16. SECURITY CLASSIFICATION OF:			17. LIMITATION OF ABSTRACT	18. NUMBER OF PAGES	19a. NAME OF RESPONSIBLE PERSON Kwok F Tom
a. REPORT	b. ABSTRACT	c. THIS PAGE	UU	70	19b. TELEPHONE NUMBER (Include area code)
Unclassified	Unclassified	Unclassified			301-394-2612

Standard Form 298 (Rev. 8/98)
Prescribed by ANSI Std. Z39.18

Contents

List of Tables

Preface

Energy detection in the RF spectrum is the most basic technique for signal detection. Typically, this requires establishing an energy detection threshold based on a noise-only condition (i.e., no signal present in the RF spectrum). Initially, the area of exploration for this report was to examine the potential of an automatic energy detection thresholding algorithm based on the RF measurement. It would not require the preliminary RF spectrum noise-only measurements to establish the energy detection threshold.

A series of RF spectrum measurements were collected at the US Army Research Laboratory in 2013. The data files contained different segments of the RF spectrum with various resolution bandwidths. In addition, the data files represented RF spectral conditions with and without RF signals. Initially, morphological imaging processing techniques were investigated to determine the potential for an automated energy detection algorithm.

The technique of "opening" was very successful in determining an energy detection threshold for the RF spectrum with signal and noise-only environments. This led to the investigation of other techniques that could be used in automated energy detection algorithms. This exploration has resulted in a series of techniques for automatic energy detection thresholding determination. This is the first of 5 reports that detail the energy detection techniques examined with the recorded RF spectrum measurements.[1–4]

---

[1] Tom K. An automated energy detection algorithm based on morphological filter processing with a semi-disk structure. Adelphi (MD): Army Research Laboratory (US); 2018 Jan. Report No.: ARL-TR-8271.

[2] Tom K. An automated energy detection algorithm based on morphological filter processing with a modified watershed transform. Adelphi (MD): Army Research Laboratory (US); 2018 Jan. Report No.: ARL-TR-8270.

[3] Tom K. An automated energy detection algorithm based on kurtosis-histogram excision. Adelphi (MD): Army Research Laboratory (US); 2018 Jan. Report No.: ARL-TR-8269.

[4] Tom K. An automated energy detection algorithm based on consecutive mean excision. Adelphi (MD): Army Research Laboratory (US); 2018 Jan. Report No.: ARL-TR-8268.

1.   Introduction

Energy detection is the simplest method of detecting a signal in the frequency spectrum. When doing so, a comparison is made between the frequency spectral component energy and a detection threshold level. Knowledge of the frequency spectrum is usually necessary to establish this detection threshold level. Various methods can be used to determine the detection threshold level, such as establishing the system noise statistics offline and setting the threshold for a given probability of detection versus probability of false alarm.

The goal of this study was to develop an algorithm that can analyze the frequency spectrum and establish a threshold value based on the spectral components. The automated processing employs techniques from image processing and statistical analysis. A combination of techniques from these 2 areas resulted in an algorithm for determining a threshold detection level. From image processing, we applied morphological filtering to the spectral data to establish a noise level. The 2 fundamental operations in this threshold-establishing algorithm are called "Erode and Dilate". This series of operations is performed on the spectral data until certain statistical criteria are met. An offset was then added to the morphological filtered data to form the threshold for energy detection.

2.   Data Collection and Statistical Summary

The local RF spectrum was measured in 2013 on the rooftop of building 204 at the US Army Research Laboratory's (ARL's) Adelphi location. An Agilent N9342CN spectrum analyzer and a Discone antenna were used to collect RF spectrum data. This spectrum analyzer was operated under the control of a LabVIEW software program to acquire and store data with different resolution bandwidth (RBW) from 1 kHz to 1 MHz.

These data files represent various sizes of RF spectral coverage from 10 MHz up to 4 GHz. The number of data files for each spectral band varied. The larger RBW files were acquired over seconds of data acquisition time versus the small RBW files. Small RBW provides fine spectral resolution, but it impacts data acquisition time for spectral coverage and data size. Depending on the RBW and spectral coverage, a data file could require a few hours of acquisition.

Table 1 summarizes the data collection measurement files. The RF spectral bands covered the spectrum from 10 MHz to 4 GHz. In general, various spectral bands were measured with 4 RBW configuration. Data file size is inversely proportional

to the RBW. Data file size is proportional to the spectral band coverage. The data size varied from approximately 1 KSample to 4 MSample data points per file.

Table 1   Summary of the RF spectrum collection

Spectral band coverage	Number of RBW measurement	RBW
1.1–1.6 GHz	4	1 kHz, 10 kHz, 100 kHz, 1 MHz
2–3 GHz	4	1 kHz, 10 kHz, 100 kHz, 1 MHz
3–4 GHz	3	10 kHz, 100 kHz, 1 MHz
4–6 GHz	3	10 kHz, 100 kHz, 1 MHz
10 MHz–1 GHz	4	1 kHz, 10 kHz, 100 kHz, 1 MHz
10 MHz–2 GHz	4	1 kHz, 10 kHz, 100 kHz, 1 MHz
10 MHz–3 GHz	4	1 kHz, 10 kHz, 100 kHz, 1 MHz
10 MHz–4 GHz	4	1 kHz, 10 kHz, 100 kHz, 1 MHz
100 MHz–1 GHz	1	100 kHz

3.   Statistical Processing

3.1 Statistical Analysis

Statistical analysis is the mathematical science dealing with the analysis or interpretation of data. The data analyst uses a few straightforward statistical techniques as a means of summarizing the collected data. These statistical techniques are under the area of descriptive statistics, which is a methodology to condense the data in quantitative terms.

In commercial prognostics and diagnostic vibrational monitoring applications, statistical techniques that are mainly used for alarm purposes in industrial plants are the statistical moments of order 2, 3, and 4. The probability density function (PDF) of the vibrational time series of a good bearing has a Gaussian distribution (also known as a normal distribution), whereas a damaged bearing results in a non-Gaussian distribution with dominant tails because of a relative increase in the number of high levels of acceleration. These techniques can be applied to the RF spectral data with a different interpretation of the results.[1]

3.1.1 Moments

If these moments are calculated about the mean, they are called central statistical moments. The first and second moments are well known, being the mean and the variance, respectively. These are analogous to the first and second area moments of inertia with the area shape defined by the PDF. The third moment is termed skewness and the fourth moment is termed kurtosis. The general equation for the order of moment is as follows:

$$M_p = \frac{1}{N} \sum_{i=1}^{N} (x_i - \bar{x})^p,$$

$where\ p\ is\ the\ order\ of\ the\ moment,$

$N\ is\ the\ number\ of\ data\ value,$

$i\ is\ the\ index\ of\ the\ data\ value, and$

$\bar{x}\ is\ the\ mean\ value\ of\ the\ data\ set.$

3.1.2 Mean

Mean is the most common measure of a statistical distribution. In this case, mean is the arithmetic average for a set of measurements.

$$\bar{x} = \mu = \frac{1}{N} \sum_{i=1}^{N} x_i .$$

3.1.3 Variance

Variance is a measure of the dispersion of a waveform about its mean—also called the second moment of the measurements.

$$\sigma^2 = \frac{1}{N} \sum_{i=1}^{N} (x_i - \bar{x})^2 .$$

3.1.4 Standard Deviation

Standard deviation is a measure of the variation of a set of data values. The standard deviation is defined as the square root of the variance moment.

$$\sigma = \sqrt{\frac{1}{N}\sum_{i=1}^{N}(x_i - \bar{x})^2}.$$

3.1.5 Kurtosis

Kurtosis is the fourth statistical moment, normalized by the standard deviation to the fourth power. It is a measure of whether the data are peaked or flat relative to a normal distribution. The noise in the RF spectrum is typically considered to have a normal distribution. The normal distribution has a value of 3.

$$\kappa = \frac{M_4}{\sigma^4}.$$

$$\kappa = \frac{\frac{1}{N}\sum_{i=1}^{N}(x_i - \bar{x})^4}{\sigma^4}.$$

$$\kappa = \frac{1}{N\sigma^4}\sum_{i=1}^{N}(x_i - \bar{x})^4.$$

3.1.6 Maximum

"Max" is the largest value of a set of numbers.

$$y = \max[x(n)].$$

3.1.7 Minimum

"Min" is the smallest value of a set of numbers.

$$y = \min[x(n)].$$

3.1.8 Median

The statistical median is an order statistic that gives the "middle" value of a set of samples. Median is the middle value of a set of data values that divides the set into 2 groups. Half the groups exist below and half exist above this value.

3.1.9 Rank Order Filter

Rank order filter is a sorting process by which a set of numbers is ordered from the smallest to the largest value. Rank order filtering is a nonlinear filtering technique that orders the contents of a filter kernel and selects the sample indexed by rank from the magnitude ordered samples.

Rank order filtering can be summarized as follows:

$$y = \sum_{i=1}^{N} a_i \tilde{x}_{(i)},$$

where $\tilde{x}_{(i)}, l = 1, \cdots, N$ is the result of sorting the data in ascending order. With this definition, the max, min, and median can be obtained from a rank order filter as follows[2]:

Min:

$$y = \sum_{i=1}^{N} a_i \tilde{x}_{(i)}$$

$$a_i = 1 \; for \; i = 1$$

$$0 \; otherwise$$

Max:

$$y = \sum_{i=1}^{N} a_i \tilde{x}_{(i)}$$

$$a_i = 1 \; for \; i = N$$

$$0 \; otherwise$$

Median:

$$y = \sum_{i=1}^{N} a_i \tilde{x}_{(i)}$$

$$a_i = 1 \; for \; i = \frac{N}{2}$$

$$0 \; otherwise$$

3.1.10 Crest Factor (CF)

Crest factor (CF) is a measure of a waveform showing the ratio of peak values to the effective value. In other words, CF indicates how extreme the peaks are in a waveform.

$$Crest\ Factor = \frac{|x|_{peak}}{x_{rms}}.$$

Noise sources are characterized by their CF, which is the peak to average ratio of the noise. In a technical bulletin, XiTRON reported CF values between 5 and 7 for random noise.[3] For example, a 5:1 CF of the noise voltage is 20log5 = 14 dB. This is a measure of the quality of the noise distributions and one way to measure its Gaussian nature.[4] For the purpose of algorithm development, the CF equation was modified as follows:

$$Crest\ Factor = \frac{Max}{Median}.$$

3.1.11 Running Median

To define the running median filter, let $\{x\}$ be a discrete time series. The running median passes a window over the sequence $\{x\}$ that selects, at each instant m, an odd number of samples to comprise the observation vector $x(n)$. The observation window is typically symmetric and centered at n, resulting in

$$x(n) = [x(n - N_1), \cdots, x(n), \cdots, x(n + N_1)]^T,$$

where N_1 may range in value over the nonnegative integers, and $N = 2N_1 + 1$ is the (odd valued) window size. While processing such noncausal observation vectors has traditionally been referred to as smoothing, we loosen the terminology somewhat and refer to the processing of both causal and noncausal observations as simply filtering. The median filter operating on the input sequence $\{x\}$ produces the output sequence $\{y\}$, where at time index n,

$$y(n) = MED[x(n)]$$

$$= Median\ value\ of\ [x(n - N_1), \cdots, x(n), \cdots, x(n + N_1)].$$

That is, the samples in the observation window are sorted, and the middle, or median, value is taken as the output.[5]

3.2 Statistical Summary

There were 31 different groupings of the RF spectrum data measurements. The number of data files under each of the main groupings was varied. For the purpose of developing the algorithm, only a single data file was selected from each group. Each data file was processed to obtain the following characteristics: RBW, mean, standard deviation, median, max, min, kurtosis, and CF. A summary of the results is in Table 2.

The following results were noted:

- The smaller the RBW, the lower the noise floor. The equation for thermal noise power is $P = kTB$, where B is bandwidth. In this case, the RBW of 1 kHz has the lowest noise value. The RBW of 1 MHz has the highest noise value.

- Each 10-fold increase in bandwidth results in a 10-dB increase in noise power. This relationship is illustrated in this data set.

- The calculated mean and median values are very close for a given RF measurement configuration.

- The CF for noise-only data files was on the order of approximately 10 to 13. Noise-only data files were estimated by visually inspecting the spectrum plot.

- The RF spectrum is not necessarily flat across the band.

Table 2   Statistical analysis of the RF spectrum measurements

Filename	Spectral Band	RBW	Mean	SD	Median	Max	Min	Kurtosis	CF
Air_test_1.1GHz_1.6GHzb_03_28_14_06_33_22	1.1 - 1.6 GHz	1000	-112.694	3.8444	-112.3	-101.2	-138.4	3.5571	11.1
Air_test_1.1GHz_1.6GHza_03_27_14_07_14_05	1.1 - 1.6 GHz	10000	-102.12	3.7226	-101.8	-91.69	-124.5	3.5134	10.11
Air_test_1.1GHz_1.6GHzc_03_31_14_06_47_26	1.1 - 1.6 GHz	100000	-90.9109	2.597	-90.75	-83.13	-101.2	3.0217	7.62
Air_test_1.1GHz_1.6GHzd_04_01_14_06_54_03	1.1 - 1.6 GHz	1000000	-80.5634	3.5741	-80.745	-55.36	-89.8	14.6861	25.385
Air_test_2GHz_3GHza_06_05_14_07_15_58	2 - 3 GHz	1000	-111.219	4.4991	-111.1	-77.55	-139	6.8918	33.55
Air_test_2GHz_3GHzb_05_29_14_06_28_28	2 - 3 GHz	10000	-101.006	4.1808	-100.8	-74.67	-122	6.1195	26.13
Air_test_2GHz_3GHzc_05_29_14_04_09_27	2 - 3 GHz	100000	-89.5666	3.4154	-89.68	-64.27	-100.3	13.2282	25.41
Air_test_2GHz_3GHzd_05_28_14_00_06_18	2 - 3 GHz	1000000	-79.6014	3.0753	-79.6	-58.74	-88.88	8.4466	20.86
Air_test_3GHz_4GHzb_06_12_14_06_30_17	3 - 4 GHz	10000	-100.51	3.7072	-100.2	-89.68	-123.7	3.5901	10.52
Air_test_3GHz_4GHzC_06_11_14_06_44_40	3 - 4 GHz	100000	-89.1625	2.5513	-89.075	-80.68	-102.3	3.0774	8.395
Air_test_3GHz_4GHzd_06_09_14_07_09_51	3 - 4 GHz	1000000	-79.0828	2.445	-78.94	-72.76	-88.5	2.9651	6.18
Air_test_4GHz_6GHza_04_24_14_07_05_26	4 - 6 GHz	1000	-107.559	4.1793	-107.2	-94.31	-136.3	3.3696	12.89
Air_test_4GHz_6GHzb_04_28_14_06_23_12	4 - 6 GHz	10000	-97.245	4.0398	-96.95	-84.05	-119.7	3.3249	12.9
Air_test_4GHz_6GHzc_04_29_14_06_48_42	4 - 6 GHz	100000	-85.9125	3.082	-85.77	-75.84	-98.78	2.9068	9.93
Air_test_10MHz_1GHza_04_17_14_07_09_30	10 MHz - 1 GHz	1000	-110.348	8.6126	-112.1	-28.37	-140.3	6.4788	83.73
Air_test_10MHz_1GHzb_04_21_14_07_17_44	10 MHz - 1 GHz	10000	-100.168	8.4775	-102	-27.95	-126.7	6.7602	74.05
Air_test_10MHz_1GHzc_04_22_14_06_39_58	10 MHz - 1 GHz	100000	-87.948	8.8113	-90.74	-27.28	-103.6	6.513	63.46
Air_test_10MHz_1GHzd_04_23_14_06_36_16	10 MHz - 1 GHz	1000000	-78.1054	8.3327	-80.59	-27.82	-89.88	7.5282	52.77
Air_test_10MHz_2GHzd_03_06_14_08_52_04	10 MHz - 2 GHz	1000	-111.275	6.9798	-112.1	-27.34	-138.3	9.5085	84.76
Air_test_10MHz_2GHzC_02_27_14_06_43_55	10 MHz - 2 GHz	10000	-100.894	7.0157	-101.8	-26.58	-125.9	10.4224	75.22
Air_test_10MHz_2GHzB_02_25_14_06_35_53	10 MHz - 2 GHz	100000	-89.242	6.7487	-90.59	-26.09	-102.4	12.7961	64.5
Air_test_10MHz_2GHz_02_20_14_06_55_36	10 MHz - 2 GHz	1000000	-78.8448	7.3203	-80.6	-26.54	-92.41	11.3819	54.06
Air_test_10MHz_3GHz_03_11_14_06_32_51	10 MHz - 3 GHz	1000	-111.373	6.1356	-111.8	-29.42	-140.5	11.0474	82.38
Air_test_10MHz_3GHzB_03_13_14_06_32_45	10 MHz - 3 GHz	10000	-100.787	6.3591	-101.4	-25.36	-125.9	11.7254	76.04
Air_test_10MHz_3GHzC_03_18_14_06_32_08	10 MHz - 3 GHz	100000	-89.1614	6.0257	-90.14	-24.16	-102.4	15.3376	65.98
Air_test_10MHz_3GHzd_03_20_14_08_09_07	10 Mhz - 3 GHz	1000000	-78.6492	6.7418	-80.8	-25.81	-90.38	13.0673	54.99
Air_test_10MHz_4GHza_04_10_14_07_01_22	10 MHz - 4 GHz	1000	-111.158	5.6813	-111.4	-28.22	-143.1	10.9573	83.18
Air_test_10MHz_4GHzb_04_11_14_06_10_18	10 MHz - 4 GHz	10000	-100.838	5.5851	-101.1	-26.85	-128	12.2576	74.25
Air_test_10MHz_4GHzc_04_15_14_07_01_09	10 MHz - 4 GHz	100000	-89.4431	5.1076	-90.03	-25.05	-103.5	18.317	64.98
Air_test_10MHz_4GHzd_04_16_14_06_42_27	10 MHz - 4 GHz	1000000	-79.0396	5.5441	-79.89	-26.72	-91.64	16.9073	53.17
Air_test_100MHz_1GHz_02_19_14_07_20_46	100 MHz - 1 GHz	100000	-88.0772	9.0701	-90.82	-23.91	-102.2	6.994	66.91

4.   Morphological Image Processing

A description of a technique for automatically estimating the noise floor spectrum was given in a conference back in 1997.[6] This technique is based on applying the morphological binary image processing operators to the RF spectrum. The technique works well in both flat and nonflat noise floor spectra. Morphology image processing is a set of nonlinear operations. Ready et al. note that "humans are good at estimating the noise floor spectrum by 'eyeballing' a spectral plot. Intuitively, we separate the spectral humps from the noise floor spectrum by eliminating those parts of the spectrum shape that are due to signals and visually draw in the noise floor spectrum."[6]

Morphology is a broad set of processing techniques that process images based on shapes. Morphological operations apply a structuring element to an input image, creating an output image of the same size. In a morphological operation, the value of each pixel in the output image is based on a comparison of the corresponding

pixel in the input image with its neighbors. By choosing the size and shape of the neighborhood, you can construct a morphological operation that is sensitive to specific shapes in the input image.

The most basic morphological operations are dilation and erosion. Dilation adds pixels to the boundaries of the objects in an image, while erosion removes pixels on object boundaries. The number of pixels added or removed from the objects in an image depends on the size and shape of the structuring element used to process the image. In the morphological dilation and erosion operations, the state of any given pixel in the output image is determined by applying a rule to the corresponding pixel and its neighbors in the input image. These rules are known as the erosion and dilation:

Erosion:

$$A \ominus B = \bigcap_{b \in B} A_{-b}.$$

Dilation:

$$A \oplus B = \bigcup_{a \in A} B_a.$$

The opening of A by B is obtained by the dilation of A by B, followed by erosion of the resulting structure by B.

Opening:

$$A \circ B = (A \ominus B) \oplus B.$$

The application of the opening technique on the RF spectrum is the basis for noise floor estimation. The estimation of the noise floor is used as a reference level to set a threshold detection level.[7]

In signal, statistical, and image processing, the minimum and maximum operators are typically encountered. Gil and Kimmel note, "In mathematical morphology, the result of such an operator is referred to as the erosion (or dilation) of the signal with a structuring element given by a pulse of width p."[8]

For the 1-D case, this reduces to a simple filter of just providing the max or min value of a set of values.[8]

1-D max filter: Given a sequence $x_0, \cdots, x_{n-1}$ and an integer $p > 1$, compute

$$y_i = \max_{0 \le j < p} x_{i+j}$$

$$\text{for} = 0, \cdots, n - p .$$

1-D min filter: Given a sequence $x_0, \cdots, x_{n-1}$ and an integer $p > 1$, compute

$$y_i = \min_{0 \le j < p} x_{i+j}$$

$$\text{For} = 0, \cdots, n - p .$$

5. Algorithm

The algorithm was originally evaluated and developed in LabVIEW. This development process was then executed in MATLAB. Appendix A is the code used to process and generate the enclosed RF spectrum signatures with the corresponding results of the morphological processing and resultant threshold detection level. The following is a description of the detection thresholding level generation based on morphological filter processing:

1) Determine the RBW of the spectral data.

2) Determine some statistics on the spectral data file: median, max, and CF.

3) Perform a sliding running median on data for a window size of 5. The start and end of the spectral data are somewhat an issue. In this case, the first 5 points used the median value determined at the first valid value. The last 5 points used the median value determined at the last valid point.

4) Perform an erosion operation on the median filtered spectral data as computed in step 3. Starting from the lowest-frequency component, create the eroded spectral array with an initial sliding window of size 2. Basically, calculate the minimum value for the given window, fill in that position, and shift the processing window one frequency position to calculate the next value. Continue on across the entire median filtered spectral data array. For the last value, use the previous valid value that is calculated.

5) Perform a dilation operation on the eroded spectral array as calculated in step 4. In this case, the calculations are performed starting at the highest frequency and continue to the lowest frequency. Dilation is simply the maximum value in the windowed data set. The initial window size is 2. In this case, the maximum value is determined from the sliding window data and used to create the dilated spectral array.

6) Calculate statistics on the dilated spectral array from step 5: mean, median, max, and CF.

7) Repeat the morphological filtering of erosion and dilation on the spectral array by increasing the window size by 1 for every pass. For example, on the second pass, the window size is 3 for erosion and dilation operations. The erosion operation is applied to the dilated spectral array from step 5. Repeat this process as long as the CF is greater than 10 and the mean power greater than 0.01 on each pass of the morphological filtering.

8) If the CF is not greater than 10, then perform the morphological filtering operations until the average power is greater than 0.01.

9) Once the convergence has been met, use the resulting morphological filtered data array (i.e., the dilated spectral array) to form the threshold as follows:

$$Threshold = Morphological\ Filtered\ Spectral\ Array + 25 - 2.9\ x\ 10\log_{10}\left(\frac{RBW}{1000}\right)$$

6. Conclusion

In general, the morphological filtering for establishing the thresholding does well.

Appendix B displays the graphs of the morphological processing for each of the selected RF spectrum data files. The red curve is the result of the morphological processing overlaid on top of the RF spectrum signature.

Appendix C displays the results of the threshold overlaid on top of the RF spectrum signature. The graphs are intended to provide the reader with a qualitative sense of the effectiveness of the automatic threshold generation algorithm. Actual processing time and the number of iterations through the morphological filtering routine are highly dependent on the RBW and spectral coverage band. A small RBW over a large coverage band requires more time to complete the process. The threshold detection level obtained works well for signals present or noise-only RF spectrum data files. The red curve is the threshold when added to the morphological processed array as shown in Appendix B.

Overall, a visual inspection of the graphs shows that the algorithm works well. The threshold parameters can be modified to obtain the desired level of detection versus the false alarm. The algorithm worked well for the RF spectrum where there are signals present as well as for the RF spectrum that was judged to be noise only.

7. References

1. Tom KF. A primer on vibrational ball bearing feature generation for prognostics and diagnostics algorithms. Adelphi (MD): Army Research Laboratory (US); 2015 Mar. Report No.: ARL-TR-7230.

2. Mitra AK, Lewis TL, Paul AS, Shaw AK. Ultra-wideband radar data models and target detection with adaptive rank-order filters. Proc SPIE 4727; 2002.

3. Crest factors and power analyzers. San Diego (CA): XiTRON Technologies; nd. Technical Brief TB 103 [accessed 2017 Nov 8]. http://www.xitrontech.com/assets/002/5788.pdf.

4. Noise: frequently asked questions. East Hanover (NJ): Noisewave; nd [accessed 2017 Nov 8]. http://www.noisewave.com/faq.pdf.

5. Barner KE, Arce GR. Order–statistic filtering and smoothing of time series: part II. In: Rao CR, Balakrishnan N, editors. Handbook of statistics. Amsterdam (Netherlands): Elsevier Science; 1998. p 555–602; (Order statistics and their applications; vol. 16).

6. Ready MJ, Downey ML, Corbalis LJ. Automatic noise floor spectrum estimation in the presence of signals. Proceedings of Thirty-First Asilomar Conference on Signals, Systems & Computers; 1997 Nov. p 877–881.

7. Sequeira S. Energy based spectrum sensing for enabling dynamic spectrum access in cognitive radios [master's thesis]. [Camden (NJ)]: Rutgers University; 2011 May.

8. Gil Y, Kimmel R. Efficient dilation, erosion, opening, and closing algorithms. IEEE Transactions on Pattern Analysis and Machine Intelligence. 2002;24(12): 1606–1617.

Appendix A. MATLAB Code

```matlab
function MorphologicalFilterROF9report()


%Make selection for data file to process
%SELECT = 1 to 31


SELECT = 15;



dir{1} = 'K:\CognitiveRadar\spectrum monitoring\data\building204-
4c085\Air_test_1.1GHz_1.6GHza\';
filename{1} = 'Air_test_1.1GHz_1.6GHza_03_27_14_07_14_05';


dir{2} = 'K:\CognitiveRadar\spectrum monitoring\data\building204-
4c085\Air_test_1.1GHz_1.6GHzb\';
filename{2} = 'Air_test_1.1GHz_1.6GHzb_03_28_14_06_33_22';


dir{3} = 'K:\CognitiveRadar\spectrum monitoring\data\building204-
4c085\Air_test_1.1GHz_1.6GHzc\';
filename{3} = 'Air_test_1.1GHz_1.6GHzc_03_31_14_06_47_26';


dir{4} = 'K:\CognitiveRadar\spectrum monitoring\data\building204-
4c085\Air_test_1.1GHz_1.6GHzd\';
filename{4} = 'Air_test_1.1GHz_1.6GHzd_04_01_14_06_54_03';


dir{5} = 'K:\CognitiveRadar\spectrum monitoring\data\building204-
4c085\Air_test_2GHz_3GHza\';
filename{5} = 'Air_test_2GHz_3GHza_06_05_14_07_15_58';


dir{6} = 'K:\CognitiveRadar\spectrum monitoring\data\building204-
4c085\Air_test_2GHz_3GHzb\';
filename{6} = 'Air_test_2GHz_3GHzb_05_29_14_06_28_28';


dir{7} = 'K:\CognitiveRadar\spectrum monitoring\data\building204-
4c085\Air_test_2GHz_3GHzc\';
filename{7} = 'Air_test_2GHz_3GHzc_05_29_14_04_09_27';


dir{8} = 'K:\CognitiveRadar\spectrum monitoring\data\building204-
4c085\Air_test_2GHz_3GHzd\';
filename{8} = 'Air_test_2GHz_3GHzd_05_28_14_00_06_18';


dir{9} = 'K:\CognitiveRadar\spectrum monitoring\data\building204-
4c085\Air_test_3GHz_4GHzb\';
filename{9} = 'Air_test_3GHz_4GHzb_06_12_14_06_30_17';


dir{10} = 'K:\CognitiveRadar\spectrum
monitoring\data\building204-4c085\Air_test_3GHz_4GHzC\';
filename{10} = 'Air_test_3GHz_4GHzC_06_11_14_06_44_40';


dir{11} = 'K:\CognitiveRadar\spectrum
monitoring\data\building204-4c085\Air_test_3GHz_4GHzd\';
filename{11} = 'Air_test_3GHz_4GHzd_06_09_14_07_09_51';
```

```
dir{12} = 'K:\CognitiveRadar\spectrum
monitoring\data\building204-4c085\Air_test_4GHz_6GHza\';
filename{12} = 'Air_test_4GHz_6GHza_04_24_14_07_05_26';


dir{13} = 'K:\CognitiveRadar\spectrum
monitoring\data\building204-4c085\Air_test_4GHz_6GHzb\';
filename{13} = 'Air_test_4GHz_6GHzb_04_28_14_06_23_12';


dir{14} = 'K:\CognitiveRadar\spectrum
monitoring\data\building204-4c085\Air_test_4GHz_6GHzc\';
filename{14} = 'Air_test_4GHz_6GHzc_04_29_14_06_48_42';


dir{15} = 'K:\CognitiveRadar\spectrum
monitoring\data\building204-4c085\Air_test_10MHz_1GHza\';
filename{15} = 'Air_test_10MHz_1GHza_04_17_14_07_09_30';


dir{16} = 'K:\CognitiveRadar\spectrum
monitoring\data\building204-4c085\Air_test_10MHz_1GHzb\';
filename{16} = 'Air_test_10MHz_1GHzb_04_21_14_07_17_44';


dir{17} = 'K:\CognitiveRadar\spectrum
monitoring\data\building204-4c085\Air_test_10MHz_1GHzc\';
filename{17} = 'Air_test_10MHz_1GHzc_04_22_14_06_39_58';


dir{18} = 'K:\CognitiveRadar\spectrum
monitoring\data\building204-4c085\Air_test_10MHz_1GHzd\';
filename{18} = 'Air_test_10MHz_1GHzd_04_23_14_06_36_16';


dir{19} = 'K:\CognitiveRadar\spectrum
monitoring\data\building204-4c085\Air_test_10MHz_2GHz\';
filename{19} = 'Air_test_10MHz_2GHz_02_20_14_06_55_36';


dir{20} = 'K:\CognitiveRadar\spectrum
monitoring\data\building204-4c085\Air_test_10MHz_2GHzB\';
filename{20} = 'Air_test_10MHz_2GHzB_02_25_14_06_35_53';


dir{21} = 'K:\CognitiveRadar\spectrum
monitoring\data\building204-4c085\Air_test_10MHz_2GHzC\';
filename{21} = 'Air_test_10MHz_2GHzC_02_27_14_06_43_55';


dir{22} = 'K:\CognitiveRadar\spectrum
monitoring\data\building204-4c085\Air_test_10MHz_2GHzd\';
filename{22} = 'Air_test_10MHz_2GHzd_03_06_14_08_52_04';


dir{23} = 'K:\CognitiveRadar\spectrum
monitoring\data\building204-4c085\Air_test_10MHz_3GHz\';
filename{23} = 'Air_test_10MHz_3GHz_03_11_14_06_32_51';


dir{24} = 'K:\CognitiveRadar\spectrum
monitoring\data\building204-4c085\Air_test_10MHz_3GHzB\';
filename{24} = 'Air_test_10MHz_3GHzB_03_13_14_06_32_45';


dir{25} = 'K:\CognitiveRadar\spectrum
monitoring\data\building204-4c085\Air_test_10MHz_3GHzC\';
```

```matlab
filename{25} = 'Air_test_10MHz_3GHzC_03_18_14_06_32_08';

dir{26} = 'K:\CognitiveRadar\spectrum
monitoring\data\building204-4c085\Air_test_10MHz_3GHzd\';
filename{26} = 'Air_test_10MHz_3GHzd_03_20_14_08_09_07';

dir{27} = 'K:\CognitiveRadar\spectrum
monitoring\data\building204-4c085\Air_test_10MHz_4GHza\';
filename{27} = 'Air_test_10MHz_4GHza_04_10_14_07_01_22';

dir{28} = 'K:\CognitiveRadar\spectrum
monitoring\data\building204-4c085\Air_test_10MHz_4GHzb\';
filename{28} = 'Air_test_10MHz_4GHzb_04_11_14_06_10_18';

dir{29} = 'K:\CognitiveRadar\spectrum
monitoring\data\building204-4c085\Air_test_10MHz_4GHzc\';
filename{29} = 'Air_test_10MHz_4GHzc_04_15_14_07_01_09';

dir{30} = 'K:\CognitiveRadar\spectrum
monitoring\data\building204-4c085\Air_test_10MHz_4GHzd\';
filename{30} = 'Air_test_10MHz_4GHzd_04_16_14_06_42_27';

dir{31} = 'K:\CognitiveRadar\spectrum
monitoring\data\building204-4c085\Air_test_100MHz_1GHz\';
filename{31} = 'Air_test_100MHz_1GHz_02_19_14_07_20_46';

str_meta =
sprintf('%s%s.mspecrawdata',dir{SELECT},filename{SELECT});
str_data =
sprintf('%s%s.specrawdata',dir{SELECT},filename{SELECT});

% Get metadata on selected data file


fid_meta = fopen(str_meta);
META = textscan(fid_meta,'%s');
ave = META{1}{1};
ref = META{1}{2};
attn = META{1}{3};
rbw = META{1}{4};

% Read in data file

fid_data = fopen(str_data);
g=0;
f=0;
a=0;
while(g==0)
    ft=fgetl(fid_data);
    f=[f,str2num(ft)];
    at=fgetl(fid_data);
    a=[a,str2num(at)];
    g=feof(fid_data);
end
```

```matlab
f=f(2:end);
a=a(2:end);

% Determine resolution bandwidth

Bandwidth = f(3) - f(2);

% Plot data file

figure(1);
plot(f/1e6,a);
axis tight;
grid;
xlabel('Frequency (MHz)');
ylabel('Power (dBm)');
title(strcat(rbw,'--',ave,'--',ref,'--
',attn),'Interpreter','none');


% Determine some statistics values for data

M = mean(a);

Med = median(a);

S = std(a);

Max = max(a);

Min = min(a);

Kurt = kurtosis(a);

Range = abs(Min - Max);

Number = floor(Range);

Bins = Number * 2;

disp([M S Med Max Min Kurt]);


% Initialize parameters

InputIndex = length(a);
ErosionIndex = 1;
InputArray = a;
ErosionArray = a;
DilationArray = a;
Medsize = 5;
Medcount = fix(Medsize);
```

```matlab
Medstart = Medcount + 1;

% Process data file with a running median

for m = Medstart:InputIndex-Medcount
    InputArray(m) = median(a(m-Medcount:m+Medcount));
end

for m = 1:Medcount
    InputArray(m) = InputArray(Medstart);
end

for m = InputIndex-Medcount:InputIndex
    InputArray(m) = InputArray(InputIndex-Medcount);
end

% Plot processed median of data file

figure(2);

plot(InputArray);

PreviousPower = sum(a)/InputIndex;

display (PreviousPower);

 % Initialize parameters

j= 1;
DiffPower = 1;

DilationMedian = Med;
DilationMax = Max;
DilationCF = DilationMax-DilationMedian;



if DilationCF > 10 && j == 1
   display('CF & Power');

% Perform Erosion operation on data file

    while DilationCF > 10

        for k = 1:InputIndex-j

         ErosionArray(k) = min(InputArray(k:k+j));

        end


        for k = InputIndex-j:InputIndex
```

```matlab
                ErosionArray(k) = InputArray(InputIndex-j);

        end


    % Plot results of Erosion operation

        figure(5);
        plot(ErosionArray);


    % Perform Dilation operation on data file

        DilationArray = ErosionArray;

            for k = InputIndex:j+1

                DilationArray(k) = max(ErosionArray(k-j:k));

            end


            for k = j:1
                    DilationArray(k) = ErosionArray(j+1);
            end

    % Plot results of Dilation operation

        InputArray = DilationArray;
        figure(6);
        plot(DilationArray);

        DilationPower = sum(DilationArray)/InputIndex;
        DilationMedian = median(DilationArray);
        DilationMax = max(DilationArray);

        DiffPower = abs(PreviousPower - DilationPower);
        DilationCF = DilationMax-DilationMedian;

        display ([j DilationPower DilationMedian DilationMax
DilationCF DiffPower]);
        PreviousPower = DilationPower;
        j= j+1;

        end

    % Check performance of the Erosion & Dilation to see if
operations
    % resulted have converged to accept criteria (If power
difference in
```

```matlab
    % the RF spectrum is less than 0.1 between iterations previous
and
    % current processing of RF spectrum

            while DiffPower > 0.1


    display('Power');



        for k = 1:InputIndex-j

            ErosionArray(k) = min(InputArray(k:k+j));

        end

        for k = InputIndex-j:InputIndex
            ErosionArray(k) = min(InputArray(k:InputIndex));
        end



    figure(5);
    plot(ErosionArray);



    DilationArray = ErosionArray;


         for k = InputIndex:j+1

            DilationArray(k) = max(ErosionArray(k-j:k));

         end

        for k = j:1
            DilationArray(k) = max(ErosionArray(k:1));
        end

    InputArray = DilationArray;
    figure(6);
    plot(DilationArray);

    DilationPower = sum(DilationArray)/InputIndex;
    DilationMedian = median(DilationArray);
    DilationMax = max(DilationArray);

    DiffPower = abs(PreviousPower - DilationPower);
    DilationCF = DilationMax-DilationMedian;
```

```
    display ([j DilationPower DilationMedian DilationMax
DilationCF DiffPower]);
    PreviousPower = DilationPower;
    j= j+1;

    end
else

    while DiffPower > 0.01

    display('Power');


        for k = 1:InputIndex-j

            ErosionArray(k) = min(InputArray(k:k+j));

        end

        for k = InputIndex-j:InputIndex
            ErosionArray(k) = min(InputArray(k:InputIndex));
        end



    figure(5);
    plot(ErosionArray);



    DilationArray = ErosionArray;


         for k = InputIndex:j+1

            DilationArray(k) = max(ErosionArray(k-j:k));

         end

        for k = j:1
            DilationArray(k) = max(ErosionArray(k:1));
        end

    InputArray = DilationArray;
    figure(6);
    plot(DilationArray);

    DilationPower = sum(DilationArray)/InputIndex;
    DilationMedian = median(DilationArray);
    DilationMax = max(DilationArray);
```

21

```matlab
        DiffPower = abs(PreviousPower - DilationPower);
        DilationCF = DilationMax-DilationMedian;

        display ([j DilationPower DilationMedian DilationMax
DilationCF DiffPower]);
        PreviousPower = DilationPower;
        j= j+1;

    end

end

 % Plot original RF spectrum and threshold

figure(3);

plot(f/1e6,a);
axis tight;

grid;
xlabel('Frequency (MHz)');
ylabel('Power (dBm)');

title(strcat(filename(SELECT),' --  ',rbw,'
Hz'),'Interpreter','none');
hold on

% Determine threshold array

Threshold = DilationArray+25-(2.9*log10(Bandwidth));


plot(f/1e6,Threshold,'r');



hold off;

% Plot original RF spectrum and final results of Erosion &
Dilation
% processing

figure(10);

plot(f/1e6,a);
axis tight;

grid;
xlabel('Frequency (MHz)');
ylabel('Power (dBm)');
```
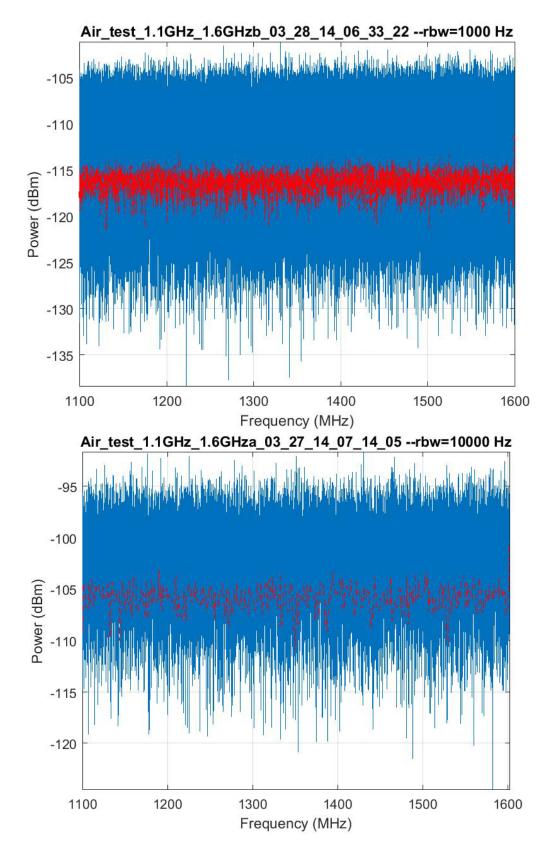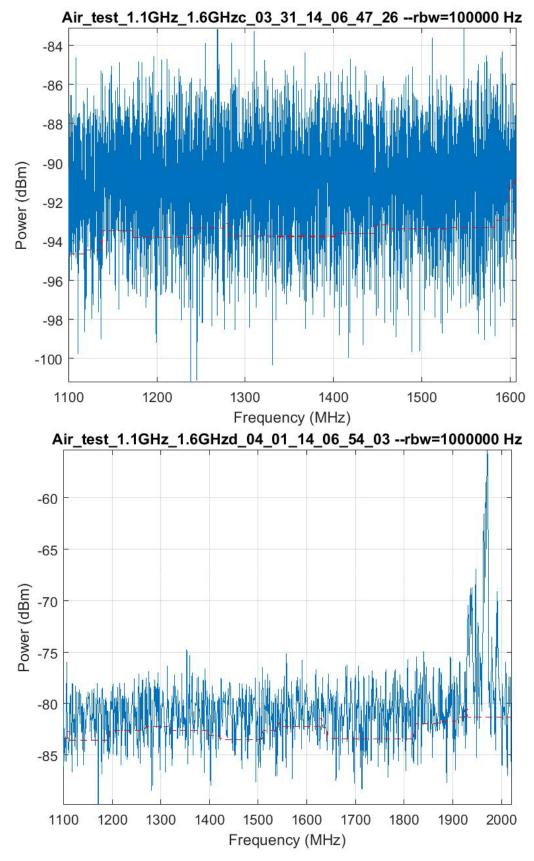
```matlab
title(strcat(filename(SELECT),' --  ',rbw,'
Hz'),'Interpreter','none');
hold on




plot(f/1e6,DilationArray,'r');




hold off;

% Save results to data file

lab = num2str(SELECT);
lab1 = strcat('ROF2-Figure ',lab,'.jpg');
saveas(gcf, lab1);

end
```
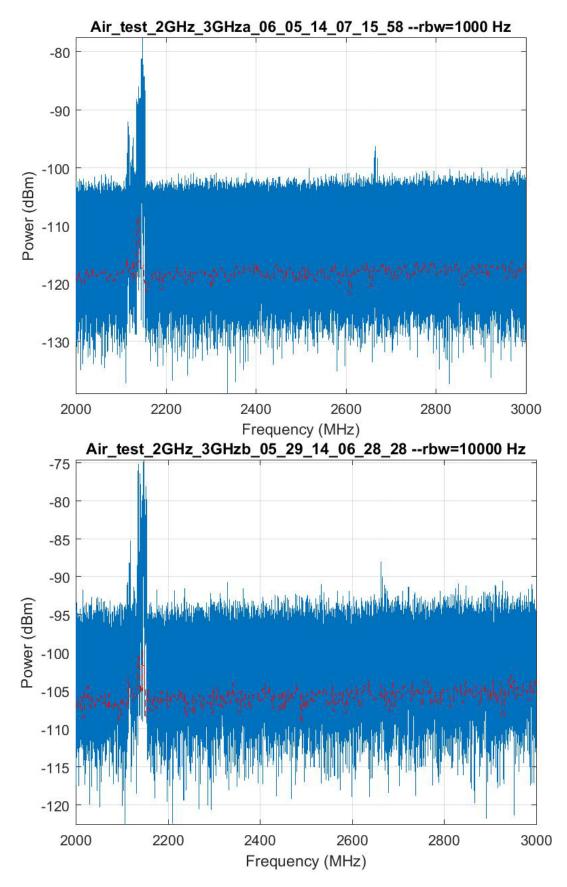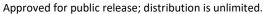
INTENTIONALLY LEFT BLANK.
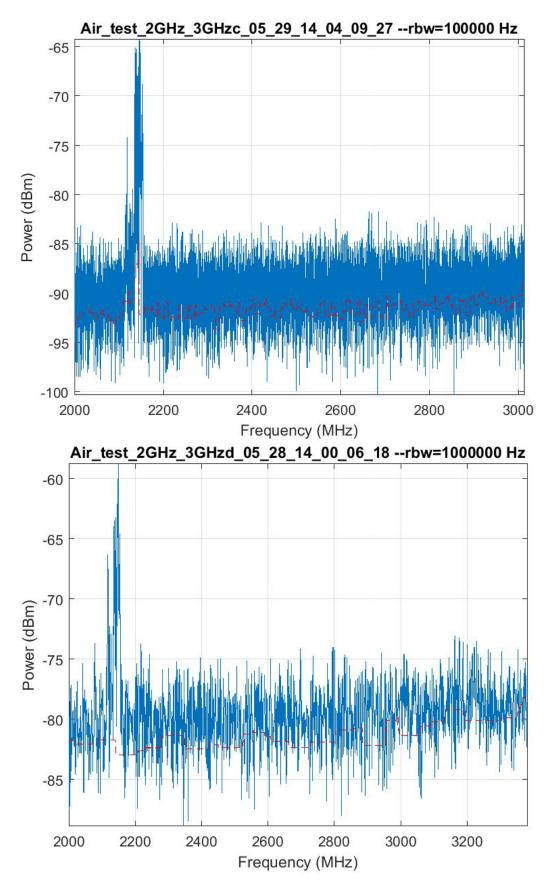
Appendix B. Graphs of Morphological Processed RF Spectrum Files

Air_test_1.1GHz_1.6GHzb_03_28_14_06_33_22 --rbw=1000 Hz

Air_test_1.1GHz_1.6GHza_03_27_14_07_14_05 --rbw=10000 Hz

Air_test_1.1GHz_1.6GHzc_03_31_14_06_47_26 --rbw=100000 Hz

Air_test_1.1GHz_1.6GHzd_04_01_14_06_54_03 --rbw=1000000 Hz

Air_test_2GHz_3GHza_06_05_14_07_15_58 --rbw=1000 Hz

Air_test_2GHz_3GHzb_05_29_14_06_28_28 --rbw=10000 Hz

Air_test_2GHz_3GHzc_05_29_14_04_09_27 --rbw=100000 Hz

Air_test_2GHz_3GHzd_05_28_14_00_06_18 --rbw=1000000 Hz

Air_test_3GHz_4GHzb_06_12_14_06_30_17 --rbw=10000 Hz

Air_test_3GHz_4GHzC_06_11_14_06_44_40 --rbw=100000 Hz

Air_test_3GHz_4GHzd_06_09_14_07_09_51 --rbw=1000000 Hz

Air_test_4GHz_6GHza_04_24_14_07_05_26 --rbw=1000 Hz

Air_test_4GHz_6GHzb_04_28_14_06_23_12 --rbw=10000 Hz

Air_test_4GHz_6GHzc_04_29_14_06_48_42 --rbw=100000 Hz

Air_test_10MHz_1GHza_04_17_14_07_09_30 --rbw=1000 Hz

Air_test_10MHz_1GHzb_04_21_14_07_17_44 --rbw=10000 Hz

Air_test_10MHz_1GHzc_04_22_14_06_39_58 --rbw=100000 Hz

Air_test_10MHz_1GHzd_04_23_14_06_36_16 --rbw=1000000 Hz

Air_test_10MHz_2GHzd_03_06_14_08_52_04 --rbw=1000 Hz

Air_test_10MHz_2GHzC_02_27_14_06_43_55 --rbw=10000 Hz

Air_test_10MHz_2GHzB_02_25_14_06_35_53 --rbw=100000 Hz

Air_test_10MHz_2GHz_02_20_14_06_55_36 --rbw=1000000 Hz

Approved for public release; distribution is unlimited.

Air_test_10MHz_3GHz_03_11_14_06_32_51 --rbw=1000 Hz

Air_test_10MHz_3GHzB_03_13_14_06_32_45 --rbw=10000 Hz

Air_test_10MHz_3GHzC_03_18_14_06_32_08 --rbw=100000 Hz

Air_test_10MHz_3GHzd_03_20_14_08_09_07 --rbw=1000000 Hz

Air_test_10MHz_4GHza_04_10_14_07_01_22 --rbw=1000 Hz

Air_test_10MHz_4GHzb_04_11_14_06_10_18 --rbw=10000 Hz

Air_test_10MHz_4GHzc_04_15_14_07_01_09 --rbw=100000 Hz

Air_test_10MHz_4GHzd_04_16_14_06_42_27 --rbw=1000000 Hz

40

Air_test_100MHz_1GHz_02_19_14_07_20_46 --rbw=100000 Hz

INTENTIONALLY LEFT BLANK.

Appendix C. Graphs of RF Spectrum Files Calculated Detection Threshold

Air_test_1.1GHz_1.6GHzb_03_28_14_06_33_22 --rbw=1000 Hz
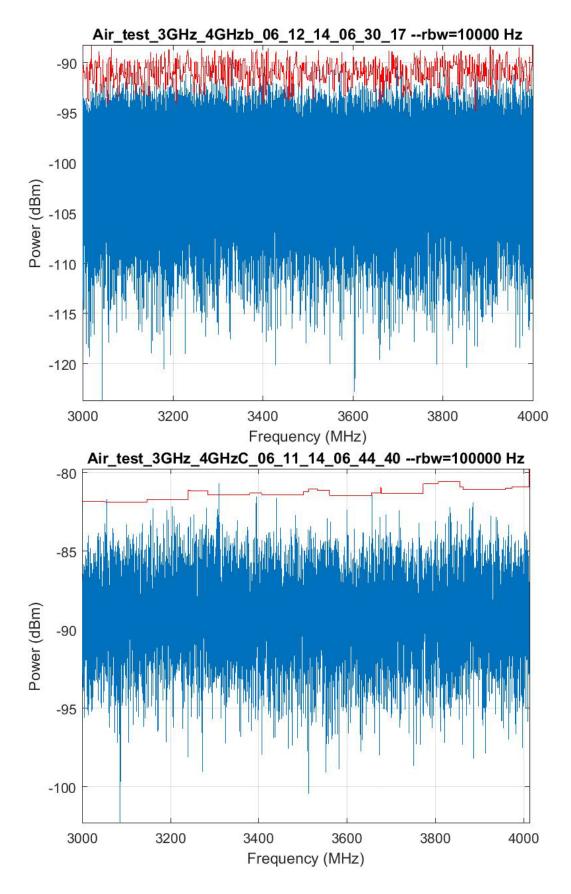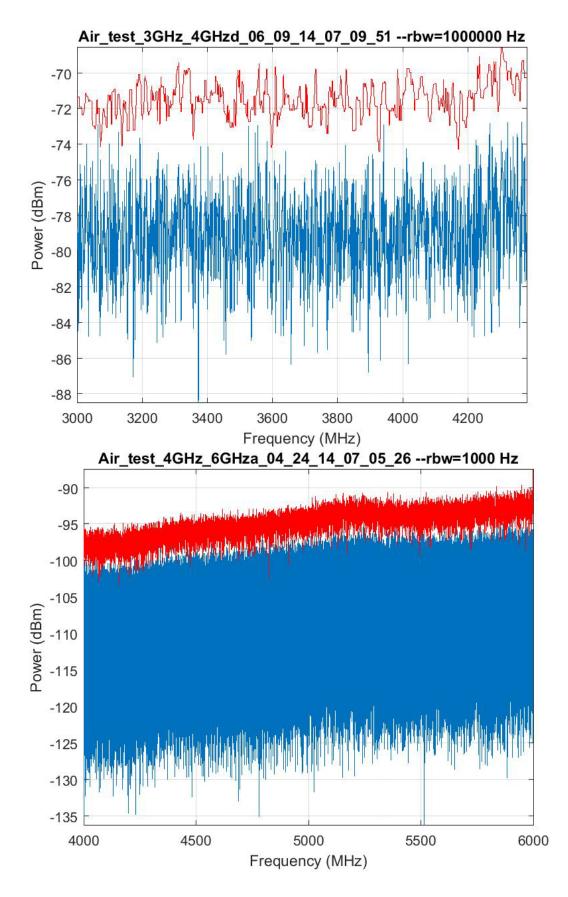
Air_test_1.1GHz_1.6GHza_03_27_14_07_14_05 --rbw=10000 Hz

Air_test_1.1GHz_1.6GHzc_03_31_14_06_47_26 --rbw=100000 Hz

Air_test_1.1GHz_1.6GHzd_04_01_14_06_54_03 --rbw=1000000 Hz

Air_test_2GHz_3GHza_06_05_14_07_15_58 --rbw=1000 Hz

Air_test_2GHz_3GHzb_05_29_14_06_28_28 --rbw=10000 Hz

Air_test_2GHz_3GHzc_05_29_14_04_09_27 --rbw=100000 Hz

Air_test_2GHz_3GHzd_05_28_14_00_06_18 --rbw=1000000 Hz

Air_test_3GHz_4GHzb_06_12_14_06_30_17 --rbw=10000 Hz

Air_test_3GHz_4GHzC_06_11_14_06_44_40 --rbw=100000 Hz

Air_test_3GHz_4GHzd_06_09_14_07_09_51 --rbw=1000000 Hz

Air_test_4GHz_6GHza_04_24_14_07_05_26 --rbw=1000 Hz

Air_test_4GHz_6GHzb_04_28_14_06_23_12 --rbw=10000 Hz

Air_test_4GHz_6GHzc_04_29_14_06_48_42 --rbw=100000 Hz

Air_test_10MHz_1GHza_04_17_14_07_09_30 --rbw=1000 Hz

Air_test_10MHz_1GHzb_04_21_14_07_17_44 --rbw=10000 Hz

Air_test_10MHz_1GHzc_04_22_14_06_39_58 --rbw=100000 Hz

Air_test_10MHz_1GHzd_04_23_14_06_36_16 --rbw=1000000 Hz

Air_test_10MHz_2GHzd_03_06_14_08_52_04 --rbw=1000 Hz

Air_test_10MHz_2GHzC_02_27_14_06_43_55 --rbw=10000 Hz

Air_test_10MHz_2GHzB_02_25_14_06_35_53 --rbw=100000 Hz

Air_test_10MHz_2GHz_02_20_14_06_55_36 --rbw=1000000 Hz

Air_test_10MHz_3GHz_03_11_14_06_32_51 --rbw=1000 Hz

Air_test_10MHz_3GHzB_03_13_14_06_32_45 --rbw=10000 Hz

Air_test_10MHz_3GHzC_03_18_14_06_32_08 --rbw=100000 Hz

Air_test_10MHz_3GHzd_03_20_14_08_09_07 --rbw=1000000 Hz

Air_test_10MHz_4GHza_04_10_14_07_01_22 --rbw=1000 Hz

Air_test_10MHz_4GHzb_04_11_14_06_10_18 --rbw=10000 Hz

Air_test_10MHz_4GHzc_04_15_14_07_01_09 --rbw=100000 Hz

Air_test_10MHz_4GHzd_04_16_14_06_42_27 --rbw=1000000 Hz

Air_test_100MHz_1GHz_02_19_14_07_20_46 --rbw=100000 Hz

List of Symbols, Abbreviations, and Acronyms

ARL   US Army Research Laboratory

CF   crest factor

GHz   gigahertz

kHz   kilohertz

MHz   megahertz

PDF   probability density function

RBW   resolution bandwidth

RF   radio frequency

1 (PDF)	DEFENSE TECHNICAL INFORMATION CTR DTIC OCA
2 (PDF)	DIR ARL IMAL HRA RECORDS MGMT RDRL DCL TECH LIB
1 (PDF)	GOVT PRINTG OFC A MALHOTRA
7 (PDF)	ARL RDRL SER E M CONN R DEL ROSARIO K F TOM D WASHINGTON RDRL SER M J SILVIOUS RDRL SER U A MARTONE RDRL SER W K RANNEY

INTENTIONALLY LEFT BLANK.